Journal of Materials Chemistry B

Accepted Manuscript

ROYAL SOCIETY OF CHEMISTRY

www.rsc.org/materialsB

Cytochrome C capped mesoporous silica nanocarriers for pH-sensitive and sustained drug release

Yuxia Tang, Ying Liu, Zhaogang Teng*, Ying Tian, Jing Sun, Shouju Wang, Chunyan Wang, Jiandong Wang, Guangming Lu*

Department of Medical Imaging, Jinling Hospital, School of Medicine, Nanjing University, Nanjing 210000, China

*Corresponding Author. Fax: +86 25 8480 4659. Tel: +86 25 8086 0185. E-mail: (Z.T.) tzg@fudan.edu.cn; (G.L.) cjr.luguangming@vip.163.com

Abstract: In this paper, pH-responsive drug nanocarriers based on mesoporous silica nanoparticles (MSNs) capped with a natural, nontoxic protein Cytochrome C (CytC) is designed and demonstrated for cancer therapy. At neutral pH the positively charged CytC can prevent the premature release of preloaded anti-cancer drug. The results show that the CytC capped nanocarriers have excellent doxorubicin (DOX) loading efficiency (414 μg mg^{-1} MSN) and the leakage of the drug is only 16% at pH 7.4 phosphate-buffered saline for 72 h. Simultaneously, DOX release percentage can reach 54% by decreasing pH to 5.5. In contrast, unsealed MSNs show a fast DOX release rate at pH 7.4 and a slight pH-response. Confocal laser scanning microscopy demonstrates that the nanocarriers can enter human breast cancer MCF-7 cells and the DOX is sustained released from the drug carriers. Cytotoxicity tests and histological assays confirm that the constructed CytC capped nanocarriers possess lower toxicity than free DOX and unsealed drug carriers. Furthermore, intratumoral administration of the nanocarriers is significantly more efficacious in tumor reduction than free DOX and unsealed drug carriers in the xenograft models of MCF-7 cancers. Overall, this study demonstrates new drug nanocarriers with pH-sensitive and sustained drug release properties

by using natural and nontoxic protein as pore blocker to achieve highly efficient cancer treatment.

Key words: Cytochome C; drug delivery; nanocarriers; mesoporous silica nanoparticle; pH-sensitive

Introduction

Mesoporous silica nanoparticles (MSNs) based drug carriers have attracted more and more attention because of their good mechanical stability, high drug loading capacity, excellent biocompatibility, and easily modified surface for targeted delivery.[1-4] More importantly, it has been reported that pharmaceutical drugs loaded in MSNs could be controlled released under different external physical/chemical stimuli, including chemicals,[5-9] temperature,[10,11] redox reactions,[12-14] and photoirradiation[15-17]. Thus, the controlled-release drug carriers present the advantageous "low premature release" property to realize drug delivery with low cytotoxicity and high therapeutic efficacy.[18,19]

Generally, the MSN-based controlled-release carriers are constructed by using different kinds of caps, such as inorganic nanoparticles,[20-23] organic molecules,[24-26] supramolecular assemblies,[27,28] or polymers[29-31] as pore blockers. Although these mesoporous silica-based nanocarriers hold promise as delivery vehicles, many of the pore-blocking agents have critical disadvantages because of their toxicity and poor biocompatibility. Therefore, the design of mesoporous silica-based drug carriers that use a natural and biocompatible component as pore blocker becomes very attractive. Very recently, mesoporous nanocarriers with nucleic acids[32] and CaP[33,34] as molecular valves have been reported for controlled-release, and recognized as valuable trials of using nontoxic molecules as pore-blocking species. These efforts toward the introduction of natural components offer useful guidance to construct new drug carriers for *in vivo* biomedical applications. Natural proteins, existing in biological body, have good biocompatibility and even metabolizable property. It would be ideal to use natural protein molecules as pore blocker agents to construct stimuli-responsive drug carriers for drug delivery. Wu et al reported that controlled release nanocarriers can be prepared by capping protein Concanavalin A on mannose ligands functionalized MSNs via carbohydrate–protein interactions.[35] However, the preparation

procedures of the stimuli-responsive nanocarriers are relatively complex and time-consuming. Therefore, it is highly desirble to construct a stimuli-responsive nanocarriers capped with protein by a ficle strategy. Cytochome C, widely existing in the cells, is a small mitochondrial protein (molecular dimensions 2.6 × 3.2 × 3.3 nm^3),[36,37] that plays a key role in cellular respiration. Recently, it was reported that CytC could be facilely loaded into MSNs and then released into the cytoplasm of cancer cells.[38] Based on the interesting results, we think the CytC is likely to be a ideal molecule to block the mesopores of MSNs for controlled drug release.

Herein, we report a novel MSN-based drug carrier by using natural protein CytC as pore blockers. The successful construction of the nanocarriers were confirmed by N_2 adsorption/desorption isotherms, Fourier-transform IR (FT-IR) spectra, and UV-Vis spectra. At neutral pH, the mesopores of MSNs are blocked with CytC to strongly inhibit the drug diffusion from the pores. At acidic pH, zeta potential changes of MSNs will promote the remove of CytC caps and allow escape of the entrapped cargos. Besides the pH-dependant controlled release, it is discovered that the CytC capped mesoporous silica nanocarriers could be internalized by MCF-7 cells and DOX could be sustained released into the cytoplasm. Moreover, relatively lower toxicity of drug loaded nanocarriers was observed based on cytotoxicity and histopathological examinations. In addition, intratumoral administration of MSN/DOX/CytC is more efficacious in tumor reduction than control groups.

Materials and methods

Materials

Analytical reagents of anhydrous ethanol, concentrated ammonia aqueous solution (25 wt %), tetraethyoxysilane (TEOS), and cetyltrimethylammonium bromide (CTAB) were purchased from Sinopharm Chemical Reagent Co., Ltd. Deionized water (Millipore) with a resistivity of

18 MΩ cm was used in all experiments. Dulbecco's Modified Eagle Media (DMEM), heat-inactivated fetal bovine serum (FBS), dimethyl sulfoxide (DMSO), and penicillin−streptomycin solution were purchased from Gibco Laboratories (Invitrogen Co, Grand Island, NY, U.S.A.). 3-(4,5-Dimethylthiazol-2-yl)-2,5-diphenyltetrazolium bromide (MTT) assay and 4'-6-diamidino-2-phenylindole (DAPI) was purchased from Nanjing Keygen Biotech. Co., Ltd. (Nanjing, China). The human breast cell MCF-7 cell line and human embryonic kidney cells (HEK293T) were obtained from American Type Culture Collection (ATCC). DOX in the form of hydrochloride salt was obtained from Beijing Huafeng United Technology Company (Beijing, China). Horse heart CytC was purchased from Sangon Biotech (Nanjing, China).

Synthesis of MSNs

MSNs were prepared *via* a surfactant-assembly sol−gel process in a Stöber solution containing CTAB, TEOS, ammonia, and ethanol according to our previous reported method.[39] Typically, CTAB was dissolved in ethanol aqueous solution containing concentrated ammonia aqueous solution (1 mL, 25 wt %). Then, the mixture was heated to 35 °C, and TEOS (1 mL) was rapidly added under vigorous stirring. The molar ratio of the reaction mixture was 1.00 TEOS: 0.394 CTAB: 2.96 NH_3: 1739 H_2O: 230 C_2H_5OH. After stirring at 35 °C for 24 h, the white product was collected by centrifugation at 12000 rpm for 10 min and washed three times with ethanol. To remove the pore-generating template (CTAB), the as-synthesized materials were transferred to an ethanol solution (120 mL) containing concentrated HCl (240 μL, 37%) and stirred at 60 °C for 3 h. The surfactant extraction step was repeated two times to ensure complete removal of CTAB. The template-removed MSNs were washed with ethanol three times and dried under high vacuum.

Construction of nanocarriers and *in vitro* drug release

Typically, 10 mg of MSNs and 5 mg of DOX were mixed within 10 mL phosphate-buffered

saline (PBS) solution. After stirring for 24 h under dark conditions, DOX loaded MSNs (denoted as MSN/DOX) were centrifuged at 12000 rpm for 10 min. To remove free DOX, the MSN/DOX were further washed three times using PBS. Then the resultant MSN/DOX was completely dissolved in 2 mL PBS. To evaluate the DOX-loading efficiency, the supernatant and washed solutions were collected and the residual DOX content was measured by using UV-Vis spectrometer at a wavelength of 490 nm. Then, 1 mL of above-prepared MSN/DOX solution was mixed with 1 mL PBS containing 0.5 mg of CytC. The mixture was allowed to stand at room temperature for 24 h under dark conditions to construct cytochrome C capped nanocarriers (denoted as MSN/DOX/CytC). Then the suspension was centrifuged for 10 min at 12000 rpm and rinsed three times using PBS to remove the free CytC. Finally, the *in vitro* simulated release of DOX from MSN/DOX/CytC was executed in pH 5.5 and 7.4 buffer solutions. In brief, the above-prepared MSN/DOX or MSN/DOX/CytC (5 mg mL^{-1}) were dissolved in 10 mL PBS solutions at 37 ℃ and shaken at 100 rpm. At certain time intervals, 0.5 mL of mixture was taken out and centrifuged to obtain a clear supernatant and analyzed using UV-Vis spectroscopy at 490 nm.

Characterization

TEM images were taken on a JEOL JEM-2100 microscope (Japan) at 200 kV. The samples were dispersed by ultrasonic in ethanol and dropped on a carbon-coated copper grid for TEM observation. X-ray power diffraction (XRD) was performed on a D8 Focus diffractometer (Bruker) with Cu Kα radiation (λ = 0.15405 nm). FT-IR spectra were recorded on a Perkin–Elmer 580B IR spectrophotometer using KBr pellet technique. N_2 adsorption/desorption isotherms were obtained on a Micromeritics ASAP 2020 M apparatus. Pore size analysis was performed by applying proper nonlocal density functional theory (NLDFT) methods from the adsorption branch of the isotherm. Zeta potential was measured by a SZ-100 nano particle analyzer (HORIBA Scientific, Tokyo, Japan). UV-Vis spectra

were obtained by a Lambda 35 UV-Vis spectrophotometer (PerkinElmer, USA). Quantitative fluorescence intensity of microscopy images were measured using Image J (NIH, Bethesda, MD). The uptake of silica species was analyzed by inductively coupled plasma-atomic emission spectroscopy (ICP-AES) using a Perkin-Elmer Optima-5300DV spectrometer.

***In vitro* cytotoxicity**

HEK293T were maintained with DMEM medium containing 10% FBS, 100 U mL^{-1} penicillin, and 100 μg mL^{-1} streptomycin at 37 °C in a humidified atmosphere with 5% CO_2. The cytotoxicity of free DOX, MSN/DOX, or MSN/DOX/CytC against HEK293T cells was evaluated by MTT assay. The cells (1×10^4 cells/well) were seeded in 96-well plates and incubated at 37 °C in 5% CO_2 atmosphere for 24 h. Then the culture medium was replaced with 100 μL of fresh medium containing varied concentration of DOX, MSN/DOX, or MSN/DOX/CytC at pH 7.4. After incubation for 12 and 24 h at 37 °C, the medium was removed and 20 μL of MTT reagent (0.5 mg mL^{-1} in culture medium) was added. Following incubation for 4 h, the MTT/medium was removed carefully and DMSO (150 μL) was added to each well for dissolving the formazan crystals. The absorbance of the solution was measured at 570 nm using a microplate reader (BioTek). Statistical analyses were performed by using SPSS version 17.0 (SPSS, Chicago, IL, USA) using Analysis of Variance (ANOVA). $P < 0.05$ was considered significant for all tests.

***In vivo* toxicity**

Animal procedures were in agreement with the guidelines of the Institutional Animal Care and Use Committee. MSN/DOX/CytC was injected into 4-week-old male, 20 g ICR mice (n = 3) at a DOX-equivalent dose of 10 mg kg^{-1} *via* the tail vein. To examine *in vivo* toxicity, the liver, spleen, heart, lung, and kidney were removed at 30 days postinjection and fixed in 10% formalin solution. Then, the tissues were embedded in paraffin, sectioned, and stained with hematoxylin and eosin. The histological sections were observed under an optical

microscope (IX71; Olympus, Tokyo, Japan). All the identity and analysis of the pathology slides were blind to the pathologist.

Measurement of the intracellular distribution of DOX

MCF-7 cells (1×10^5 cells mL^{-1} per well) were seeded onto a cover glass-bottom dish in 2 mL of DMEM supplemented with 10% FBS, 1% antibiotics (penicillin 100 U mM^{-1}, streptomycin 0.1 mg mL^{-1}). After incubation for 24 h (37 °C, 5% CO_2), the medium was carefully aspirated and replaced with 1 mL of medium containing 5 μg mL^{-1} DOX equivalent of MSN/DOX and MSN/DOX/CytC. The cells were incubated for 2 and 12 h, and then washed three times with PBS and stained with DAPI. The confocal laser scanning microscopy (CLSM) images of MCF-7 cells were obtained using a confocal laser scanning microscope (FV1000, Olympus Corporation, Germany) by blue fluorescing (λex = 405 nm) and red-fluorescing (λex = 480 nm). The cells in twelve-well plates (1×10^5 cells/well) were incubated with 1 mL of medium containing 100 μg mL^{-1} MSN equivalent of MSN/DOX and MSN/DOX/CytC for 12 h. To observe the MSN/DOX and MSN/DOX/CytC, the cells were washed with PBS and immediately fixed with 2.5% glutaraldehyde in PBS. After secondary fixation in 1% OsO_4 in PBS, cells were dehydrated in a graded ethanol series, treated with propylene oxide, and embedded in resin. Approximately 60–70 nm thick sections were cut with a Leica ultramicrotome and supported on Formvar-coated copper grids. Sections were examined on a JEOL JEM-2100 TEM (Japan). To evaluate the contents of silica species, the cells were washed with PBS three times and collected for ICP-AES measurements.

Therapeutic efficacy

To generate a subcutaneous mouse model, a suspension of 5×10^6 MCF-7 breast cancer cells in PBS (100 μL) was inoculated into the subcutaneous dorsa of female athymic nude mice (5 weeks old, 18–22 g, five mice per group). When the tumor volume was approximately 250 to 300 mm^3, saline, free DOX, MSN/DOX, and MSN/DOX/CytC were administrated by

intratumoral injection at a DOX-equivalent dose of 10 mg kg^{-1}. The tumor size was calculated as $a \times b^2/2$, where a was the largest and b the smallest diameter. Tumors were dissected from MCF-7 tumor-bearing mice on day 30 after treatment. The tumor sizes treated by MSN/DOX and MSN/DOX/CytC were analyzed by using SPSS version 17.0 (SPSS, Chicago, IL, USA) using Student's t test. $P < 0.05$ was considered significant for all tests.

Results and discussion

The design of the CytC-gated nanocarriers is depicted in Fig. 1a. Firstly, MSNs synthesized by the Stöber method were loaded with DOX. Secondly, MSN/DOX was further placed in CytC solution (pH 7.4). Due to CytC is positively charged in the near neutral solution, the CytC can caped on the DOX loaded MSNs through ion exchange process to block the mesopores. Finally, the *in vitro* release behavior of DOX from MSN/DOX/CytC was evaluated at pH 7.4 and pH 5.5, respectively. TEM images show that the prepared mesoporous silica nanoparticles are nearly spherical in shape (Fig. 1b) with radially orientated channels (Fig. 1c) and average diameters of 117 ± 10 nm (Fig. S1). The XRD pattern shows a typical 100 peak of hexagonal structure, indicating their ordered mesostructure (Fig. 1d). The nitrogen sorption analysis of MSNs exhibits a type IV isotherm (Fig. 2a). The BET surface area and pore volume of the MSNs are calculated to be as high as of 797 $m^2\ g^{-1}$ and 0.67 $cm^3\ g^{-1}$, respectively. The NLDFT method gave one pore size distribution centered on 3.2 nm (Fig. 2a, inset). Upon loading with DOX the BET surface area decreased to 404 $m^2\ g^{-1}$ and the pore volume reduced to 0.4 $cm^3\ g^{-1}$. After capped with CytC, the BET surface area and the pore volume further reduced to 142 $m^2\ g^{-1}$ and 0.2 $cm^3\ g^{-1}$, respectively. These changes in the results of nitrogen sorption analysis confirm the successful loading of DOX and capping of CytC. The loading efficiencies of DOX in MSN/DOX and MSN/DOX/CytC are measured to be as high as 414 μg DOX per milligram

of MSNs. The zeta potentials of MSNs were also measured to confirm the construction of the drug delivery nanocarriers. The results show that the zeta potentials of pure MSNs are –14.4 mV at pH 7.4 and –0.496 mV at pH 5.5, respectively (Fig. 2b). Thus, at pH 7.4, the positively charged DOX can bind with the negatively charged MSNs to form MSN/DOX complex by electrostatic interaction,[40] which can enhance the drug loading efficiency. On the other hand, the zeta potentials of MSN/DOX, and MSN/DOX/CytC are measured to be 26.2 and 30.5 mV (Fig. 2b), respectively, obviously suggesting that the loading of DOX and capping of CytC were successful. Besides, FT-IR spectroscopy was obtained to characterize the samples. The spectrum of bare MSNs shows only the surface silanol groups and low-frequency silica vibrations. The emerging absorption band at around 1700 cm^{-1} on the FT-IR spectrum of MSN/DOX can be assigned to C=O stretching of carboxyl groups[41] contained within the adsorbed DOX, and the amide I bands at around 1653 cm^{-1} on the spectrum of MSN/DOX/CytC supported the capping of CytC (Fig. 2c).[42] Consistently, UV-Vis spectrum of MSN/DOX/CytC displays both the characteristic DOX peak at 490 nm[43] and CytC peak at 409 nm[38] (Fig. 2d).

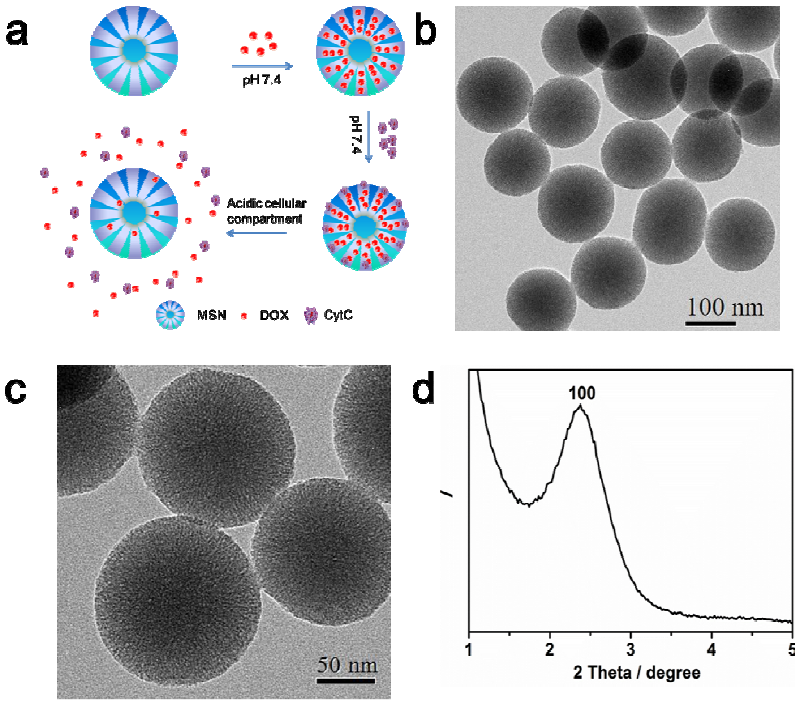

Fig. 1 (a) Schematic illustration of the construction of the CytC capped nanocarriers. TEM images of MSNs at (b) low and (c) high magnification, and (d) XRD pattern of MSNs.

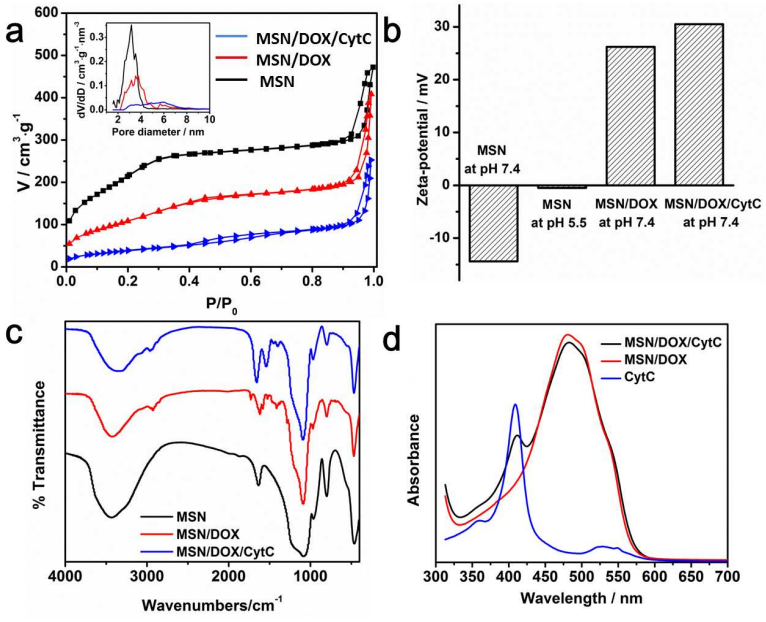

Fig. 2 (a) Nitrogen sorption isotherms and the pore size distribution curves (inset) of the

MSNs, MSN/DOX and MSN/DOX/CytC. (b) Zeta potentials of MSNs, MSN/DOX and MSN/DOX/CytC in PBS. (c) FT-IR spectra of MSNs, MSN/DOX and MSN/DOX/CytC. (d) UV-Vis spectra of MSN/DOX/CytC, MSN/DOX and CytC dispersed in PBS.

Definitely, drug release is an important parameter for drug delivery. The release profiles of MSN/DOX and MSN/DOX/CytC were measured at pH values of 7.4 and 5.5 for 72 h at 37 °C. Fig. 3 demonstrates that unsealed MSN/DOX presents a fast DOX release rate with a slight pH-responsive, which is consistent with the results previously reported in literature.[44] The fast drug release is attributed to that the MSN/DOX lacks the pore-blocking species, thus DOX could not be effectively prevented. As a comparison, the DOX release rate from MSN/DOX/CytC is obviously pH dependent and increases with the decrease of pH value. At pH 7.4, the release amount from MSN/DOX/CytC is quite low and only approximately 16% is released after 72 h. At pH 5.5, a faster release behavior is observed and the release amount reaches 54% after 72 h, which is almost three times of that at pH 7.4. Therefore, MSN/DOX/CytC displays a more pronounced pH dependent property than MSN/DOX, and more drug molecules could be released for MSN/DOX/CytC system at lower pH solution. Then we further prolonged the DOX release time from MSN/DOX and MSN/DOX/CytC to 120 h. The release of drug reached equilibrium after 72 h and the final release amount of drug is about 54% (Fig. S2). Besides, ibuprofen was loaded into the drug carriers and the drug release profiles also show pH-responsive property (Fig. S3). Considering the fact that the tumor tissues are more acidic than the normal tissues,[45] the prepared MSN/DOX/CytC nanocarriers would be able to release drug in the tumor tissues on demand with little premature release to minimize the side effects of DOX. Combined with the specific pH responsive drug release behavior and high loading capacity (414 μg mg^{-1} MSN), the MSN/DOX/CytC are highly expected to be used in cancer treatment without frequent interval

medication administrations.

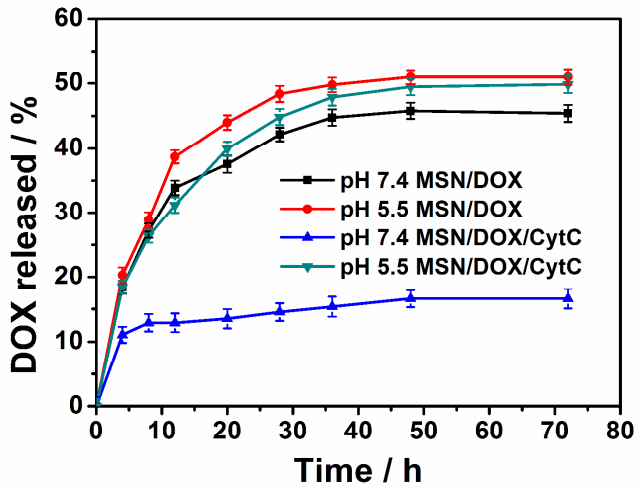

Fig. 3 DOX release profiles from MSN/DOX and MSN/DOX/CytC at pH 7.4 and pH 5.5.

The drug distribution of free DOX, MSN/DOX, and MSN/DOX/CytC in MCF-7 cells was monitored by CLSM. The nucleus was labeled with DAPI as an indicator. After 2 h of incubation, MCF-7 cells treated with free DOX exhibited a bright red fluorescence within nuclei (Fig. 4a), while MSN/DOX and MSN/DOX/CytC exhibited a bright red fluorescence within the cytoplasm, but a negligible DOX fluorescence within nuclei (Fig. 4b and d). After a further 10 h of incubation, a strong fluorescence was found in nuclei (Fig. 4c and e), which can be attributed to the released DOX from MSN/DOX or MSN/DOX/CytC. By further analysis of fluorescence intensity profiles of fluorescence images of 30 cells (Fig. S4), it can be easily observed that MSN/DOX/CytC showed a weaker red fluorescence within nuclei than MSN/DOX even after 12 h of incubation, indicating that DOX release from MSN/DOX/CytC is slower. TEM images were also taken to investigate the uptake of the drug-loaded nanocarriers in the cells. After 12 h, MSN/DOX or MSN/DOX/CytC could be found in cytoplasm (Fig. S5). At the same time, the quantitative analysis of cellular uptake of MSN/DOX and MSN/DOX/CytC were studied by ICP-AES test. After incubated with 100 μg

mL^{-1} MSN equivalent of MSN/DOX and MSN/DOX/CytC for 12 h, the average concentrations of intracellular silica species were 50.8 ± 4 and 71.2 ± 5 μg mL^{-1}, respectively. These results indicated that the weaker fluorescence of the cells treated with MSN/DOX/CytC is from the slower drug release, not from the lower cellular uptake of the drug-loaded nanocarriers. Thus, the sustained release can achieve a long period of drug release and maintain an adequate blood concentration.

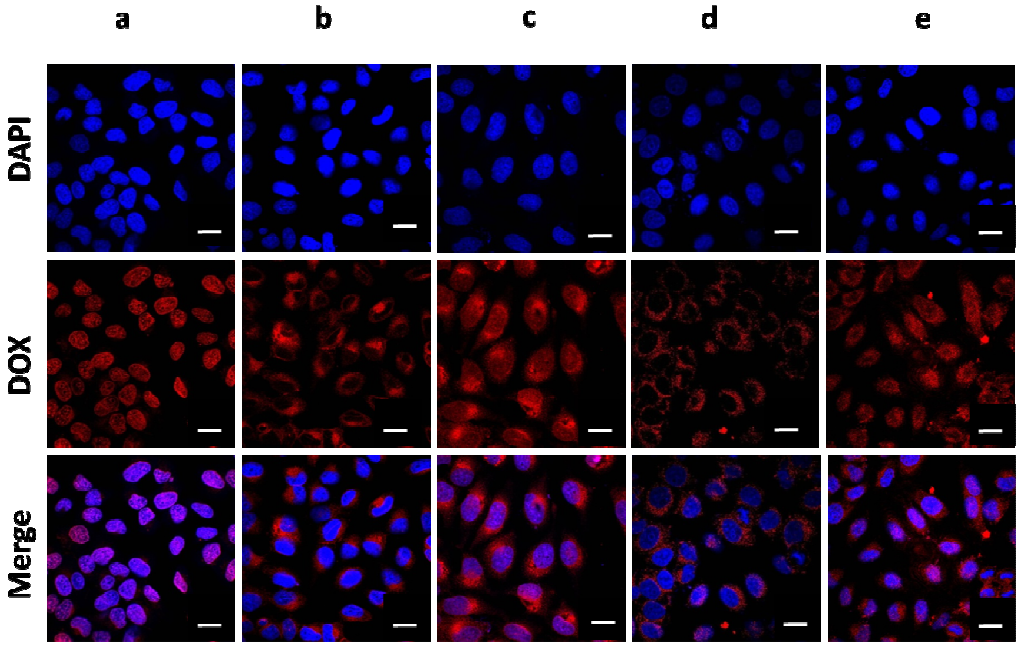

Fig. 4 CLSM images of live MCF-7 cells treated with free DOX, MSN/DOX, and MSN/DOX/CytC (DOX = 5 mg mL^{-1}). (a) Free DOX for 2 h exposure, (b) MSN/DOX for 2 h exposure, (c) MSN/DOX for 12 h exposure, (d) MSN/DOX/CytC for 2 h exposure, and (e) MSN/DOX/CytC for 12 h exposure. (Blue fluorescence is associated with DAPI; the red fluorescence is expressed by free DOX, released DOX, and DOX retained within MSN.) Scale bar: 20 μm.

The pH dependent and sustained release profiles of the nanocarriers motivated us to further investigate their toxicity. The cytotoxicity of free DOX, MSN/DOX, and MSN/DOX/CytC to

HEK293T cells was investigated by MTT assay. As shown in Fig. 5a and b, when HEK293T cells were incubated with 0.5, 1.0, 2.0, 4.0, 8.0 μg mL^{-1} of DOX-equivalent dose for 12 h, the somewhat lower toxicity of MSN/DOX/CytC compared to free DOX and MSN/DOX, and the same trend was observed with the time prolonged to 24 h. Statistical analysis by ANOVA indicated that the cell viability average change caused by MSN/DOX/CytC were statistically higher than those by MSN/DOX in each condition (Table S1). These results were deduced due to the gradual release of DOX for MSN/DOX/CytC within the cells and entered the nucleus more slowly. Hence, the MSN/DOX/CytC nanocarriers may minimize side effect of drugs in physiological blood and have potential applications in clinical chemotherapy. Histological assessment was further used to investigate the toxicity of the MSN/DOX/CytC. Analysis was performed on the tissues obtained from the harvested organs (liver, heart, lung, spleen, and kidney). As shown in Fig. 5c, hepatocytes in the liver samples appear normal, and there are no inflammatory infiltrates and steatosis. Cardiac muscle tissue in the heart samples shows no hydropic degeneration. No pulmonary fibrosis and inflammation are observed in the lung samples. No apparent tissue injury, inflammation, lesions, or necrosis is observed in the other organs. These results indicate that CytC possess an excellent efficiency for capping the pores and decreasing the rate of drug leakage in blood.

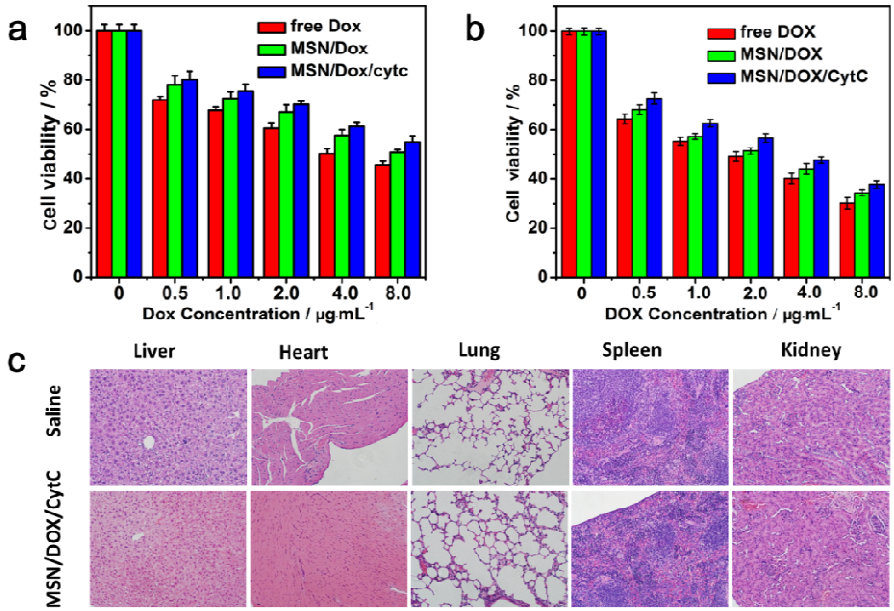

Fig. 5 *In vitro* viability of human embryo kidney 293T cells incubated with free DOX, MSN/DOX, and MSN/DOX/CytC for (a) 12 h and (b) 24 h. (c) Representative tissue sections of mice stained with hematoxylin and eosin. All images shown here are 200× magnifications.

We next evaluated the *in vivo* efficacy of MSN/DOX/CytC using xenograft models of MCF-7 human breast cancers. As illustrated in Fig. 6a, MSN/DOX/CytC can delivery DOX to a tumor through enhanced permeability and retention (EPR) effects. Then the anti-cancer drugs are controlled released within endosomes and lysosomes, corresponding to local pH values between 5 and 6. Fig. 6b shows that the treatments with free DOX and MSN/DOX were also effective in tumor regression to some extent, but did not show a comparable efficacy to MSN/DOX/CytC. Statistical analyses of tumor sizes treated by MSN/DOX and MSN/DOX/CytC showed that there was significant difference of the tumor volumes between the two groups ($P = 0.034$). So the tumor size is indeed smaller treated by MSN/DOX/CytC compared to MSN/DOX, indicating a better inhibition of tumor growth. One reason for the enhanced *in vivo* efficacy might be the delayed clearance of MSN/DOX/CytC at the tumor site because of the retention property of the nanoparticles. In addition, CytC could protect

DOX against rapid clearance before endocytosis and the subsequent intracellular release of DOX may contribute to the enhanced antitumor effect. This is possibly as a result of the small size of free DOX or extracellularly released DOX from MSN/DOX that would be rapidly diffused away from the tumor interstitium.

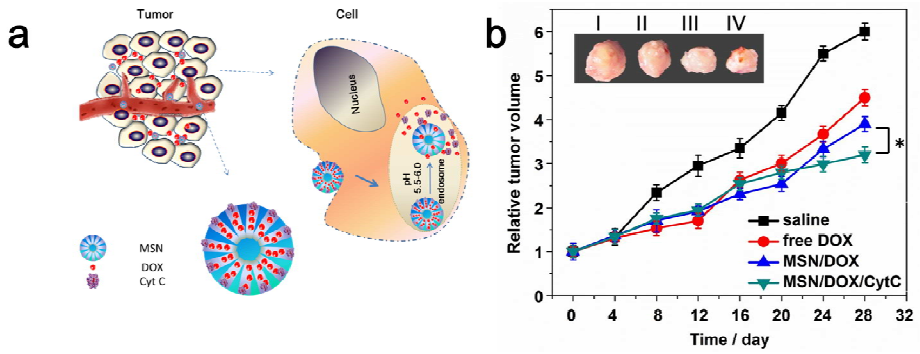

Fig. 6 (a) Schematic of MSN/DOX/CytC and triggered drug release under intracellular endo/lysosomal and tumor conditions. (b) *In vivo* therapeutic efficacy after intratumoral injection of saline, free DOX, MSN/DOX, and MSN/DOX/CytC at a DOX-equivalent dose of 10 mg kg^{-1}. Inset: images of excised tumors after 30 days post-treatment. I: saline, II: free DOX, III: MSN/DOX, IV: MSN/DOX/CytC.

Conclusion

In conclusion, we have demonstrated that the introduction of CytC as a natural, nontoxic pore blocker on the MSN surfaces provides a novel route for smart mesoporous silica nanocarriers. The attachment of CytC not only protects the DOX in physiological condition (pH 7.4) but effectively allows the sustained-release of the drugs in acidic environment (pH 5.5). *In vitro* cytotoxicity tests with HEK293T cells and histological assays confirm that the obtained CytC capped nanocarriers exhibit low toxicity. Moreover, CytC capped drug carriers have an enhanced efficiency in tumor inhibition were also demonstrated. Overall, this study provides MSN based naonocarriers with pH-sensitive and sustained drug release properties

by using nontoxic, natural CytC as pore blocker for cancer therapy.

Acknowledgments

We greatly appreciate financial support from the National Key Basic Research Program of the PRC (2014CB744504), the National Natural Science Foundation of China (81201175 and 81371611), the National Key Basic Research Program of the PRC (2011CB707700), the Major International (Regional) Joint Research Program of China (81120108013), and the National Science Foundation for Post-doctoral Scientists of China (2012M521934 and 2013T60939).

References

1. C. Coll, A. Bernardos, R. Martinez-Manez and F. Sancenon, *Acc. Chem. Res.*, 2013, 46, 339–349.
2. Z. Li, J. C. Barnes, A. Bosoy, J. F. Stoddart and J. I. Zink, *Chem. Soc. Rev.*, 2012, 41, 2590–2605.
3. S. H. Wu, Y. Hung and C. Y. Mou, *Chem. Commun.*, 2011, 47, 9972–9985.
4. J. E. Lee, N. Lee, T. Kim, J. Kim and T. Hyeon, *Acc. Chem. Res.*, 2011, 44, 893–902.
5. Y. Zhao, B. G. Trewyn, Slowing, II and V. S. Lin, *J. Am. Chem. Soc.*, 2009, 131, 8398–8400.
6. X. He, Y. Zhao, D. He, K. Wang, F. Xu and J. Tang, *Langmuir*, 2012, 28, 12909–12915.
7. Z. Zhang, D. Balogh, F. Wang and I. Willner, *J. Am. Chem. Soc.*, 2013, 135, 1934–1940.
8. C. S. Yeh, C. H. Su, W. Y. Ho, C. C. Huang, J. C. Chang, Y. H. Chien, S. T. Hung, M. C. Liau and H. Y. Ho, *Biomaterials*, 2013, 34, 5677–5688.
9. I. Candel, E. Aznar, L. Mondragon, C. de la Torre, R. Martinez-Manez, F. Sancenon, M. D. Marcos, P. Amoros, C. Guillem, E. Perez-Paya, A. Costero, S. Gil and M. Parra, *Nanoscale*, 2012, 4, 7237–7245.

10. J. T. Sun, Z. Q. Yu, C. Y. Hong and C. Y. Pan, *Macromol. Rapid Commun.*, 2012, 33, 811–818.
11. Z. Chen, Z. M. Cui, C. Y. Cao, W. D. He, L. Jiang and W. G. Song, *Langmuir*, 2012, 28, 13452–13458.
12. X. Wan, D. Wang and S. Liu, *Langmuir*, 2010, 26, 15574–15579.
13. W. Xia, X. Y. Hu, Y. Chen, C. Lin and L. Wang, *Chem. Commun.*, 2013, 49, 5085–5087.
14. T. D. Nguyen, Y. Liu, S. Saha, K. C. Leung, J. F. Stoddart and J. I. Zink, *J. Am. Chem. Soc.*, 2007, 129, 626–634.
15. D. He, X. He, K. Wang, J. Cao and Y. Zhao, *Langmuir*, 2012, 28, 4003–4008.
16. J. L. Vivero-Escoto, Slowing, II, C. W. Wu and V. S. Lin, *J. Am. Chem. Soc.*, 2009, 131, 3462–3463.
17. D. P. Ferris, Y. L. Zhao, N. M. Khashab, H. A. Khatib, J. F. Stoddart and J. I. Zink, *J. Am. Chem. Soc.*, 2009, 131, 1686–1688.
18. D. Peer, J. M. Karp, S. Hong, O. C. Farokhzad, R. Margalit and R. Langer, *Nat. Nanotechnol.*, 2007, 2, 751–760.
19. W. X. Mai and H. Meng, *Integr. Biol.*, 2013, 5, 19–28.
20. Z. Teng, X. Zhu, G. Zheng, F. Zhang, Y. Deng, L. Xiu, W. Li, Q. Yang and D. Zhao, *J. Mater. Chem.*, 2012, 22, 17677–17684.
21. R. Liu, Y. Zhang, X. Zhao, A. Agarwal, L. J. Mueller and P. Feng, *J. Am. Chem. Soc.*, 2010, 132, 1500–1501.
22. E. Aznar, M. D. Marcos, R. Martinez-Manez, F. Sancenon, J. Soto, P. Amoros and C. Guillem, *J. Am. Chem. Soc.*, 2009, 131, 6833–6843.
23. F. Muhammad, M. Guo, W. Qi, F. Sun, A. Wang, Y. Guo and G. Zhu, *J. Am. Chem. Soc.*, 2011, 133, 8778–8781.
24. C. L. Zhu, C. H. Lu, X. Y. Song, H. H. Yang and X. R. Wang, *J. Am. Chem. Soc.*, 2011, 133, 1278–1281.
25. A. Bernardos, E. Aznar, M. D. Marcos, R. Martinez-Manez, F. Sancenon, J. Soto, J. M. Barat and P. Amoros, *Angew. Chem. Int. Ed.*, 2009, 48, 5884–5887.

26. M. Chen, C. Huang, C. He, W. Zhu, Y. Xu and Y. Lu, *Chem. Commun.*, 2012, 48, 9522–9524.

27. C. Park, K. Oh, S. C. Lee and C. Kim, *Angew. Chem. Int. Ed.*, 2007, 46, 1455–1457.

28. R. Klajn, J. F. Stoddart and B. A. Grzybowski, *Chem. Soc. Rev.*, 2010, 39, 2203–2237.

29. N. Singh, A. Karambelkar, L. Gu, K. Lin, J. S. Miller, C. S. Chen, M. J. Sailor and S. N. Bhatia, *J. Am. Chem. Soc.*, 2011, 133, 19582–19585.

30. A. Bernardos, L. Mondragon, I. Javakhishvili, N. Mas, C. de la Torre, R. Martinez-Manez, F. Sancenon, J. M. Barat, S. Hvilsted, M. Orzaez, E. Perez-Paya and P. Amoros, *Chemistry*, 2012, 18, 13068–13078.

31. L. Xing, H. Zheng, Y. Cao and S. Che, *Adv. Mater.*, 2012, 24, 6433–6437.

32. C. Chen, F. Pu, Z. Huang, Z. Liu, J. Ren and X. Qu, *Nucleic Acids Res.*, 2011, 39, 1638–1644.

33. H. P. Rim, K. H. Min, H. J. Lee, S. Y. Jeong and S. C. Lee, *Angew. Chem. Int. Ed.*, 2011, 50, 8853–8857.

34. Z. Chen, Z. Li, Y. Lin, M. Yin, J. Ren and X. Qu, *Biomaterials*, 2013, 34, 1364–1371.

35. S. Wu, X. Huang and X. Du, *Angew. Chem. Int. Ed.*, 2013, 52, 5580–5584.

36. M. Hartmann, *Chem. Mater.*, 2005, 17, 4577–4593.

37. H. M. Berman, J. Westbrook, Z. Feng, G. Gilliland, T. N. Bhat, H. Weissig, I. N. Shindyalov and P. E. Bourne, *Nucleic Acids Res.*, 2000, 28, 235–242.

38. Slowing, II, B. G. Trewyn and V. S. Lin, *J. Am. Chem. Soc.*, 2007, 129, 8845–8849.

39. J. Wang, Z. Teng, Y. Tian, T. Fang, J. Ma, J. Sun, F. Zhu, J. Wu, X. Wang, N. Yang, X. Zhou, S. Yun and G. Lu, *J Biomed. Nanotechnol.*, 2013, 9, 1882–1890.

40. I. Slowing, J. Viveroescoto, C. Wu and V. Lin, *Adv. Drug Deliv. Rev.*, 2008, 60, 1278–1288.

41. C. M. Popescu and B. C. Simionescu, *Appl. Spectrosc.*, 2013, 67, 606–613.

42. J.-H. Choi, S. Ham and M. Cho, *J. Chem. Phys.*, 2002, 117, 6821–6832.

43. J. Fan, F. Zeng, S. Wu and X. Wang, *Biomacromolecules*, 2012, 13, 4126–4137.

44. H. Meng, M. Liong, T. Xia, Z. Li, Z. Ji, J. I. Zink and A. E. Nel, *ACS Nano*, 2010, 4, 4539–4550.

45. R. J. Gillies, N. Raghunand, M. L. Garcia-Martin and R. A. Gatenby, *IEEE Eng. Med. Biol. Mag.*, 2004, 23, 57–64.

Graphical Abstract:

Cytochrome C capped mesoporous silica nanocarriers for pH-sensitive and sustained drug release

Yuxia Tang, Zhaogang Teng*, Ying Liu, Ying Tian, Jing Sun, Shouju Wang, Chunyan Wang, Jiandong Wang, Guangming Lu*

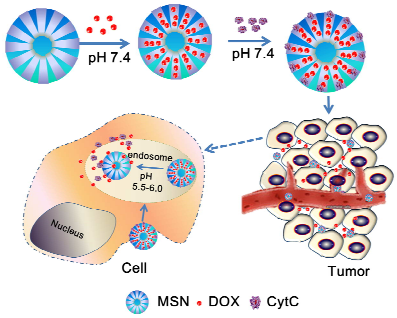

Drug nanocarriers with pH-sensitive and sustained drug release properties were constructed by using Cytochrome C as pore blocker to achieve high therapeutic efficacy for cancer.